Check for updates

Received: 29 April 2020 | Revised: 23 January 2021 | Accepted: 7 April 2021

DOI: 10.1002/jnm.2888

SPECIAL ISSUE PAPER

WILEY

Artificial intelligence–based design optimization of nonuniform microstrip line band pass filter

Tarlan Mahouti[1] | **Tülay Yıldırım**[2] | **Nilgün Kuşkonmaz**[1]

[1]Department of Metallurgy and Material Science, Yıldız Technical University, Istanbul, Turkey

[2]Department of Electronics and Communications Engineering, Yıldız Technical University, Istanbul, Turkey

Correspondence
Tarlan Mahouti, Department of Metallurgy and Material Science, Yıldız Technical University, Istanbul, Turkey.
Email: tarlan.mahouti@gmail.com

Abstract

Design optimization of many electromagnetic and multiphysics problems have multiscale issues that require a fast, efficient, and accurate surrogate-based model to be used. Recently, in microwave engineering field, artificial intelligence–based models are being used for modeling of complex microwave stages. In all the studies, the main aim is to form models inner structure parameters, by using the given data to predict the linear/nonlinear relationships between given inputs and outputs. Herein, a surrogate-based model of a nonuniform microstrip transmission line (NTL) with a typical application of design optimization of a band-pass filter for ISM band application using deep learning (DL) and meta-heuristic optimization has been presented. In order to have a computationally efficient and accurate optimization process, firstly a 3D EM unit element model of NTL has been designed. The training and test data sets are created based on different sampling methods. A DL regression model modified multilayer perceptron M2LP have been used for prediction of scattering parameters (S) of the NTL, with respect to the variation of geometrical design parameters. The proposed S-parameters will then be used to calculate the equivalent S-parameters of the cascading NTL to be used to calculate the NTL-based microstrip band-pass filter S-parameter response. The optimal design parameters of each line used in the filter design have been determined using a fast and powerful optimization algorithm differential evolutionary algorithm.

KEYWORDS

band pass filter, deep learning, multiobjective optimization, nonuniform transmission lines, regression, surrogate-based modeling

1 | INTRODUCTION

Design optimization of many electromagnetic and multiphysics problems has multiscale issues that require a fast, efficient, and accurate surrogate-based model to be used. Similar to any typical RF device, microstrip circuit designs are also in need of design optimization process. With the increase in the aimed performance criteria's like being wideband, low loss small in size, and so forth, the design process would become even more complex. At this stage, a challenging problem for designers is that they made a choice between using a coarse surrogate model to have computationally efficient optimization process at the cost of accuracy and using a fine 3D electromagnetic simulation–based design model with high accuracy at cost of having very low or infeasible computation efficient design optimization process.[1]

 © 2021 John Wiley & Sons Ltd.

In recent years, in order to achieve the challenging problem of highly aggregated simulation cost, many studies had been presented. One of the proposed efficient solution methods is utilization of surrogate models of studied problems with faster computationally abilities.[2-7] One of the surrogate modeling classes is approximation also known as data-driven models.[3] This method is based on approximating sampled simulation data which provides advantages such as no need of expert knowledge of the studied problem, ability of adaptation between problems and applications, high computational efficiency, and so forth.[8-10] Some of the commonly applied approximation/data-driven models can be named as kriging,[11,12] radial basis functions (RBF),[13] Gaussian process regression (GPR),[14] neural networks,[6,15-17] support vector regression,[18,19] polynomial response surfaces,[20] or fuzzy models.[21]

The data given to surrogate models are usually obtained with a help of 3D EM simulation tool or via measured characteristics. The most crucial step in design of surrogate models is to provide sufficient training samples of the model. The shortcoming of surrogate models is their weakness to the impact of dimensionality on their performance with the increase in number of variables, their variation range, and total sample size; these models might become inefficient or not feasible, due to the need of high amount of samples, to be used.[2,22]

Thus, another challenging problem here is to have a properly created data set that is not only computational efficient but also should be informatively sufficient enough for the surrogate model to create a mapping between the design variables such as operation frequency, geometrical design parameters such as width, length, and so forth, spacing, or placement configuration of element/elements in the design, with the mentioned output characteristics. Even though the gathering process is time consuming and requires a substantial effort, once the training of the surrogate model is finished, the total computation time of simulation/prediction can be negated, most specially in cases of repeated design analysis or design optimization process.[2,23]

Some of the related work in literature on surrogate-based modeling of microwave circuits and their applications can be named as follows: estimation of microwave transistors performance characteristics,[24-28] prediction of reflection phase characteristic of reflect array antennas unit elements,[29-31] for synthesis and analysis of microstrip lines,[32-34] for estimation of a microstrip patch antenna's resonant frequency and modeling of microstrip antennas,[35,36] scattering parameter and frequency identification method for ANN-based eye-height/width prediction,[37] computationally feasible narrowband antenna,[38] and design optimization of microwave antenna designs.[39-43]

In this work, as shown in Figure 1, it is aimed to propose a surrogate model of a nonuniform microstrip transmission line with a typical application of design optimization of a band-pass filter for ISM band application using deep learning (DL) and meta-heuristic optimization algorithms. In order to have a computationally efficient and accurate optimization process, firstly, a 3D EM unit element model of transmission line has been designed. The training and test data sets are generated based on different sampling methods. A regression model modified multilayer perceptron (M2LP)[44] had been used for prediction of scattering [S] parameters of the NTL, with respect to the variation of geometrical design parameters. Furthermore, the performance of the proposed M2LP model has been compared with counterpart regression model, and as a result, it found that the proposed method is more accurate in means of cross validation and hold out performances. The predicted scattering parameters will then be used to calculate the equivalent S parameters of the cascaded transmission lines that will be used to calculate the NTL-based microstrip band-pass filter scattering parameter against the frequency response. The optimal design parameters of each line used in the filter design have been determined using a fast and powerful meta-heuristic optimization algorithm and differential evolutionary optimization algorithm. Finally, the numerical results obtained from the proposed M2LP-based design optimization method have been justified with 3D EM simulation tool CST. In the next section, design process of unit NTL element and proposed NTL microstrip band-pass filter have been presented alongside of the required data set for forming the M2LP-based regression model. In Section 3, a study case on the design optimization process of NTL microstrip band-pass filter

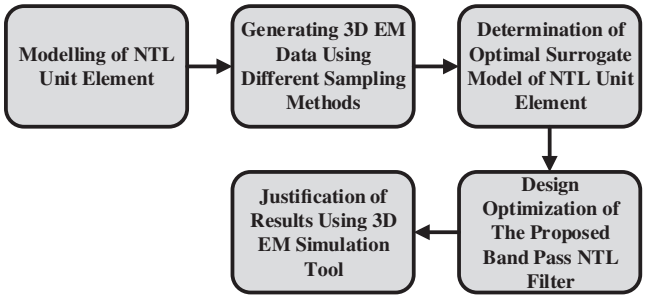

FIGURE 1 Flowchart of the proposed work

using meta-heuristic optimization algorithm and M2LP-based regression model have been presented. Finally, work ends with a brief conclusion section.

2 | DESIGN PROCESS

2.1 | Modeling of unit element

In Figure 2, schematic of nonuniform transmission line (NTL) is presented. Herein, it is meant to create a black-box model of the proposed NTL in order to predict the S parameters of this two-port passive circuit element with respect to the variation of geometrical parameters such as widths and lengths.

The proposed unit NTL element will be used in cascade form as given in Figure 3, to form a microstrip band-pass filter as a case study. It should be mentioned that, once the proposed model is achieved, this NTL can be used for design optimization of other type of microwave circuits, such as other type of filters, impedance matching circuits, power dividers, and so forth; however, it should be noted that although the proposed NTL is usable in all mentioned design optimization problems, the cost function and the cascaded configuration matrixes should be adjust accordingly. Figure 3 shows the schematic of a symmetrical 7 element microstrip filter. Here, in order to avoid the coupling effect between unit elements, the transmission lines input and output sections width (w_1) is taken equal as 1 mm, for all elements. Thus, during the calculation of equivalent S-parameters, the effect of coupling in unit elements had been minimized.

2.2 | Creation of training and test dataset

Among the circuit parameters, S-parameters are the most common ones to be used in the microwave literature since they can be determined by direct measurements. Another feature of the scattering parameters is that the S-matrix elements fall against sizes of physical importance. That is, when other ports are terminated without reflection, the diagonal elements of the matrix determine the reflection coefficients for the respective gate, and the nondiagonal elements determine the transmission coefficients between the doors to which they belong. Scatter parameters in microwave circuits can be easily measured with circuit (Network) analyzers developed for this purpose.

In this sub-section, the procedure of creating 3D EM-based training and test datasets has been presented. 3D EM simulation tool CST has been used to create simulated results of scattering [S] parameters of the NTL unit element. As mentioned before, in order to avoid the coupling effect between the junctions of unit elements in cascade, configuration (w_1) is taken as a constant value. Thus, other design parameters can be taken as the optimization variables. In Figure 4, the effect of selected design variables of NTL unit element over the NTL's scattering parameters characteristic has been presented.

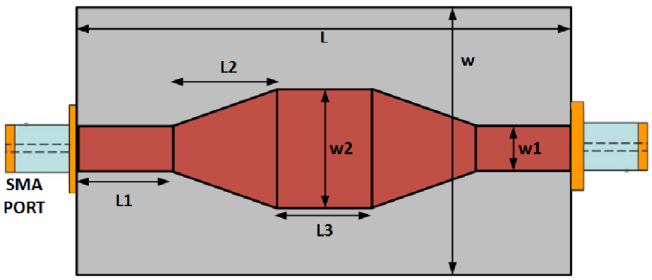

FIGURE 2 Schematic of unit element nonuniform transmission line

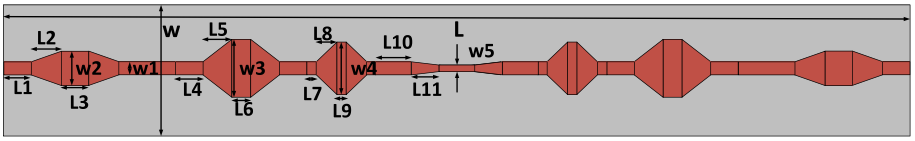

FIGURE 3 Schematic of symmetrical 7 element NTL microstrip filter

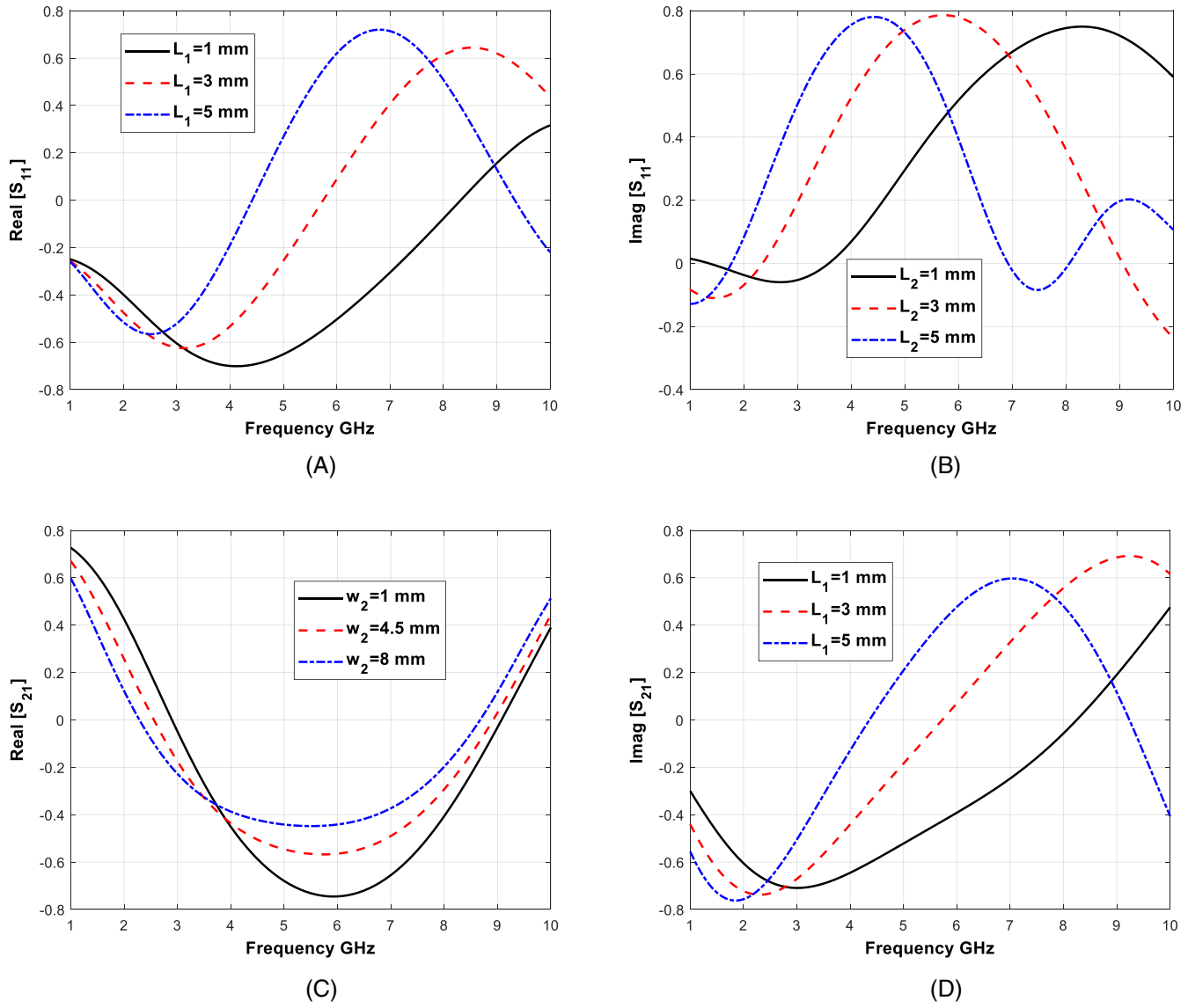

FIGURE 4 Scattering parameter response of NTL with respect to variation of design parameters

TABLE 1 Search domain of the NTL unit element

Parameter	Range	Sampling method	Number of samples (Excluding frequency points)
L_1 (mm)	1–5	Data set 1: Latin hypercube	216
L_2 (mm)	1–5	Data set 2: Linear (6 point)	216
w_2 (mm)	1–15	Data set 3: Logarithmic (6 point)	216
Frequency (GHz)	1–10	Data set 4: Random	300

As can be seen from Figure 4, each of the design variables can affect the scattering parameter response of unit element, while all the other variables are constant. Thus, in order to have a numerical model to precisely predict the characteristic response of unit element with variation of each geometrical design parameter, a dataset is required. In Table 1, different sampling methods have been used for generating training and test data for a computationally efficient optimization procedure. The effectiveness of each sampling methods for the creating the proposed M2LP-based NTL (Figure 5) will be tested based on a cross-validation method ($k = 5$) and a hold-out data set (data set 4).

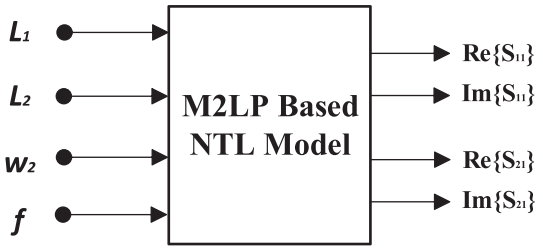

FIGURE 5 Black box model of the proposed M2LP-based NTL

It should be mentioned that, w_1 is taken as 1 mm constant, L_3 is taken equal as half of L_2, and the material used as substrate is taken as FR4 (1.6 mm with dielectric constant of 4.6, loss tangent 0.035). Each training sample comes with 91 frequency samples in the frequency range of 1–10 GHz.

Since the proposed NTL design is a reciprocal circuit ($S_{ij} = S_{ji}$, i and $j = 1, 2$), by only calculating S_{11} and S_{21} characteristics, other scattering parameters can be obtained. Thus, in the black-box model (Figure 5), only real and imaginary parts of S_{11} and S_{21} are taken as outputs.

3 | CASE STUDY

3.1 | M2LP-based modeling

The first application of DL algorithms had been started with image processing applications, where these algorithms achieved outstanding results compared to their counterpart methods. Nowadays, DL algorithms had become a new trending solution method for solving challenging problems in many fields such as segmentation,[45,46] multiobject tracking,[47,48] biomedical applications,[49,50] lip reading,[51] activity recognition of humans via mobile sensors,[52] remaining life estimation of subsystems via sensor data,[53] estimation of time series of financial data,[54] power and speed estimation of wind,[55,56] electrical impedance tomography (EIT) imaging,[57] full-wave nonlinear inverse scattering problems,[58] large-scale offline signature recognition,[59] high-speed receiver adaptation,[60] parametric modeling, and extraction of passive microwave components.[7,61]

Modified multilayer perceptron (M2LP) had been proposed by Calik et al.[44] as a fast and accurate regression method for modeling the scattering parameters of a capacitive-feed antenna model to be used in design optimization problems. M2LP is based on a standard multilayer perceptron (MLP), where instead of traditional parameters of MLP such as "sigmoid" and "tanh" as for activation functions, Levenberq Marquardt, Bayesian regression, and so forth methods as for training the models, more advanced design parameters of deep learning algorithms such as batch norm layer, leaky ReLU, parametric ReLU, and Adam training algorithm specifically developed for training of accurate models have been used. Other user defined parameters have been presented in Table 2.

$$\mathrm{MAE} = \frac{1}{N}\sum_{i=1}^{N}|T_i - P_i|, \tag{1}$$

$$\mathrm{SMAPE} = \frac{100}{N}\sum_{i=1}^{N}\frac{|T_i - P_i|}{(|T_i| + |P_i|)/2}. \tag{2}$$

T is targeted real/imaginary value of S_{11}, and P is predicted real/imaginary value of S_{11} using M2LP. Here, it should be noted that during the presentation of model performance results, the given MAE and SMAPE values are the mean values of real and imaginary S_{11}, N is the total number of samples; here it should be noted that for each of the data sets in Table 1, the N is equal to the number of mentioned data set multiplied by 91 for frequency samples. For an example, the total number of samples in data set 4 is equal to 27 300 ($N = 300 \times 91 = 27\,300$). In Equations (1) and (2), the error metrics of mean absolute error (MAE) and symmetric mean absolute percentage error (SMAPE) are used for determination of estimation performance of the proposed model for real and imaginary parts of scattering parameters of the NTL. Since NTL is a reciprocal two port model, for complete S parameter modeling, only S_{21} and S_{11} are required. In Table 3, the minimum, maximum, and mean performance results of each of data sets are presented for different architectures of

Learning rate	$[10^{-2}, 10^{-5}]$ exp decay
Batch size	500
Weight init.	Xavier Improved
Optimizer	Adam
Weight decay	10^{-5}
Loss function	MAE
Epoch	250

TABLE 2 User defined parameters Of M2lp

M2LP for 10 different runs. Also, the obtained values belong to the mean error of both real and imaginary part of S_{11} characteristic. A model with architecture parameters of "M-N" means that the model has N neurons in its first layer with the depth of M. Here, standard deviation is obtained from the results of each run of cross-validation ($K = 5$). Furthermore, for the evaluation of over-fitting of models, Dataset 4 has been used as hold out data set. The performance results of each model for holdout data are also given in Table 3.

As can be seen from Table 3, M2LP model with depth of 2 and first layer neuron size of 64 achieved the best overall performance MEA and SMAPE for the holdout dataset. Furthermore, in Table 4, performance comparison of the selected M2LP model with counterpart regression methods has been presented. Each of the models is trained using data set 3 with a $k = 5$ fold cross-validation process; also their performance has been further investigated with holdout data set using SMAPE error metric. Based on the results from Table 4, it can be said that the proposed M2LP model with the depth of 2 and first layer neuron size of 64 trained with Dataset 3 is shown a great performance without failing into over-fitting error. Thus, from now on, this model will be used for design optimization process of the proposed M2LP-based NTL band-pass filter.

3.2 | Design optimization of an M2LP-based band-pass NTL filter

Here, the M2LP-based unit NTL element will be used to form a symmetrical 7 element microstrip filter for ISM band applications. The proposed 7 element NTL filter is formed via cascade configuration of M2LP-based NTL elements. In this symmetrical model, there will be total of four different NTL elements. Thus, the design of the NTL filter would consists of 12 variables that each would directly affect the S characteristics (S_{21}, S_{11}) of the filter based on the black box model of NTL given in Figure 5. Hence, the proposed design optimization problem is a multiobjective multidimension problem which requires an objective function (Equations (3)–(6)) to optimally determine the values of each cascaded NTL. In Figure 6, the flowchart of the optimization process is given.

$$\text{Objective} = \text{Cost}_1 + \text{Cost}_2 + \text{Cost}_3, \tag{3}$$

$$\text{Cost}_1 = \sum_{f=f_a}^{f_{c_1}} \left[S_{21}(f) + \left(\frac{1}{S_{11}(f)} - 1 \right) \right], \tag{4}$$

$$\text{Cost}_2 = \sum_{f=f_{c_1}}^{f_{c_2}} \left[S_{11}(f) + \left(\frac{1}{S_{21}(f)} - 1 \right) \right], \tag{5}$$

$$\text{Cost}_3 = \sum_{f=f_{c_2}}^{f_b} \left[S_{21}(f) + \left(\frac{1}{S_{11}(f)} - 1 \right) \right], \tag{6}$$

f_a and f_b are the minimum and maximum frequency values of the analyzed band, and f_c represents the cut-off frequency of the NTL filter. In this work, these values are taken as $f_a = 1$ GHz, $f_b = 5$GHz, and f_{c1} and f_{c2} as 2.2 GHz and 2.7 GHz, respectively. The aim of cost functions, 1 and 3, is to reject the incoming EM signals between the stated frequencies,

TABLE 3 Performance results of the M2LP model for all data sets

			Training			Hold-out		
Training data set	**Architecture parameter**	**Error metric**	**Max**	**Min**	**Mean**	**Max**	**Min**	**Mean**
Data set 1	2–16	MAE $\times 10^{-3}$	14.51	13.318	13.85	26.57	24.89	25.62
		SMAPE	2.86	2.72	2.81	5.27	5.06	5.16
	2–32	MAE $\times 10^{-3}$	11.41	10.92	11.13	22.13	21.14	21.46
		SMAPE	2.41	2.33	2.36	4.518	4.40	4.44
	2–64	**MAE $\times 10^{-3}$**	**11.58**	**9.84**	**10.45**	**20.44**	**18.85**	**19.38**
		SMAPE	**2.46**	**2.12**	**2.24**	**4.34**	**4.02**	**4.14**
	3–16	MAE $\times 10^{-3}$	12.46	11.61	12.04	23.66	22.37	22.87
		SMAPE	2.56	2.41	2.47	4.76	4.53	4.61
	3–32	MAE $\times 10^{-3}$	11.19	10.54	10.87	20.23	19.66	19.90
		SMAPE	2.36	2.21	2.28	4.24	4.13	4.18
	3–64	MAE $\times 10^{-3}$	11.06	10.27	10.69	20.19	19.58	19.87
		SMAPE	2.46	2.21	2.30	4.38	4.17	4.25
Data set 2	2–16	MAE $\times 10^{-3}$	12.98	12.52	12.80	20.41	19.72	20.02
		SMAPE	3.08	2.94	3.00	4.01	3.92	3.97
	2–32	MAE $\times 10^{-3}$	9.66	9.07	9.36	15.41	14.43	15.12
		SMAPE	2.39	2.26	2.32	3.20	3.06	3.17
	2–64	**MAE $\times 10^{-3}$**	**9.081**	**8.50**	**8.80**	**14.36**	**13.00**	**13.78**
		SMAPE	**2.24**	**2.18**	**2.20**	**3.09**	**2.90**	**2.98**
	3–16	MAE $\times 10^{-3}$	10.56	10.29	10.40	16.59	15.84	16.11
		SMAPE	2.56	2.50	2.53	3.42	3.34	3.36
	3–32	MAE $\times 10^{-3}$	10.31	9.01	9.59	14.68	14.04	14.32
		SMAPE	2.49	2.26	2.36	3.180	3.01	3.09
	3–64	MAE $\times 10^{-3}$	9.88	8.96	9.41	14.53	13.31	13.76
		SMAPE	2.48	2.26	2.36	3.165	2.97	3.02
Data set 3	2–16	MAE $\times 10^{-3}$	13.48	12.72	13.18	15.29	14.57	14.99
		SMAPE	2.94	2.77	2.87	3.28	3.11	3.21
	2–32	MAE $\times 10^{-3}$	10.11	9.26	9.71	11.94	11.32	11.66
		SMAPE	2.32	2.19	2.26	2.65	2.52	2.60
	2–64	**MAE $\times 10^{-3}$**	**9.41**	**8.76**	**9.12**	**11.39**	**11.02**	**11.17**
		SMAPE	**2.20**	**2.08**	**2.17**	**2.56**	**2.46**	**2.51**
	3–16	MAE $\times 10^{-3}$	11.59	10.71	11.07	13.53	12.69	13.05
		SMAPE	2.58	2.43	2.50	2.91	2.77	2.83
	3–32	MAE $\times 10^{-3}$	9.51	9.25	9.37	11.87	11.06	11.55
		SMAPE	2.32	2.17	2.22	2.63	2.51	2.57
	3–64	MAE $\times 10^{-3}$	9.92	9.12	9.50	12.34	11.62	11.93
		SMAPE	2.34	2.18	2.25	2.75	2.60	2.64

Note: Highlighted model is the model with best performance result for the selected data set.

while cost function 2 is intended to transfer all the incoming EM signals in the given band to form a band-pass filter. All the frequency values or their numbers (designing multiband pass filters) can be determined by the need of the designer; however, it should be noted that with respect to the complexity, the NTL filter must be adjusted with increasing the number of element. Each S-parameter of NTL element will be predicted by M2LP to be used for calculation of equivalent S parameter of 7 element NTL filter (Figure 7) by using Equations (7)–(10).[62]

TABLE 4 Performance comparison of the best selected models of m2lp and counterpart methods after 10 different runs using smape metric

Method	Data set 3	Holdout
Autotuned K-nearest neighbors regressor (Euclidean distance)	10.59	10.63
Gradient boosted trees regressor with early stopping (Least-squares loss)	8.38	7.96
Nystroem Kernel SVM regressor	9.48	6.47
M2LP 2–64	**2.08**	**2.46**

Bold value indicates minimum value in the table.

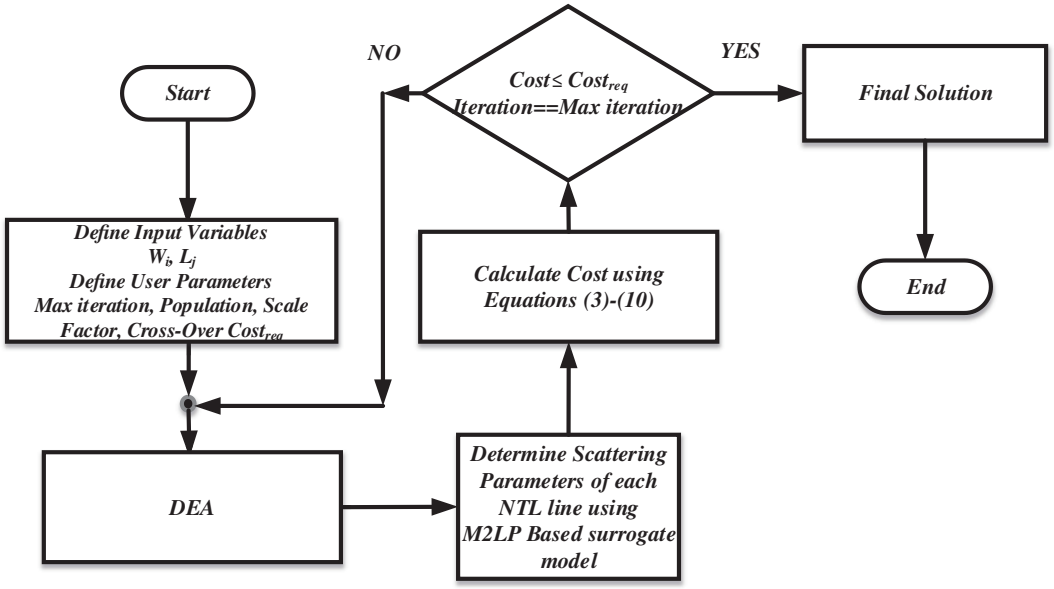

FIGURE 6 Flowchart of design optimization process of NTL band-pass filter using DEA- and M2LP-based surrogate model

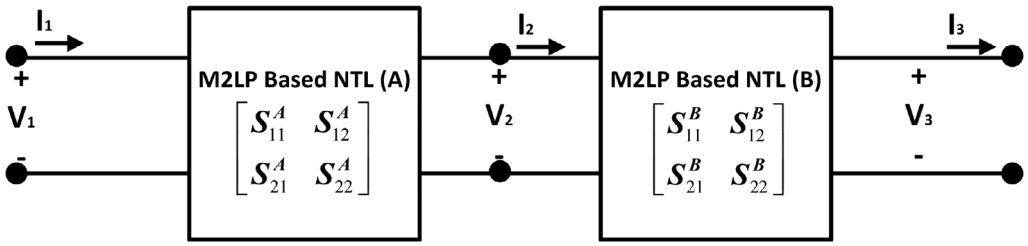

FIGURE 7 Cascade configuration of two M2LP NTL

$$S_{11} = S_{11}{}^{A} + \frac{S^{A}{}_{12} S_{11}{}^{B} S_{21}{}^{A}}{1 - S_{22}{}^{A} S_{11}{}^{B}}, \tag{7}$$

$$S_{12} = \frac{S^{A}{}_{12} S_{12}{}^{B}}{1 - S_{11}{}^{B} S_{22}{}^{A}}, \tag{8}$$

$$S_{21} = \frac{S_{21}{}^{B} S_{21}{}^{A}}{1 - S_{22}{}^{A} S_{11}{}^{B}}, \tag{9}$$

$$S_{22} = S_{22}{}^{B} + \frac{S_{21}{}^{B} S_{22}{}^{A} S_{12}{}^{B}}{1 - S_{11}{}^{B} S_{22}{}^{A}}. \tag{10}$$

TABLE 5 Optimal geometrical design parameters of 7 element NTL filter (mm)

L_1	4.15	L_{10}	1.3
L_2	4.6	L_{11}	4.75
L_4	0.55	w_2	1.85
L_5	4.35	w_3	11.56
L_7	0.95	w_4	14.2
L_8	2.8	w_5	1.5

FIGURE 8 3D model of the optimally designed 7 element NTL filter

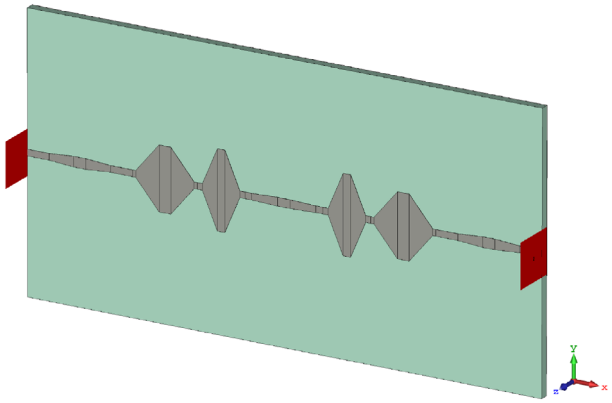

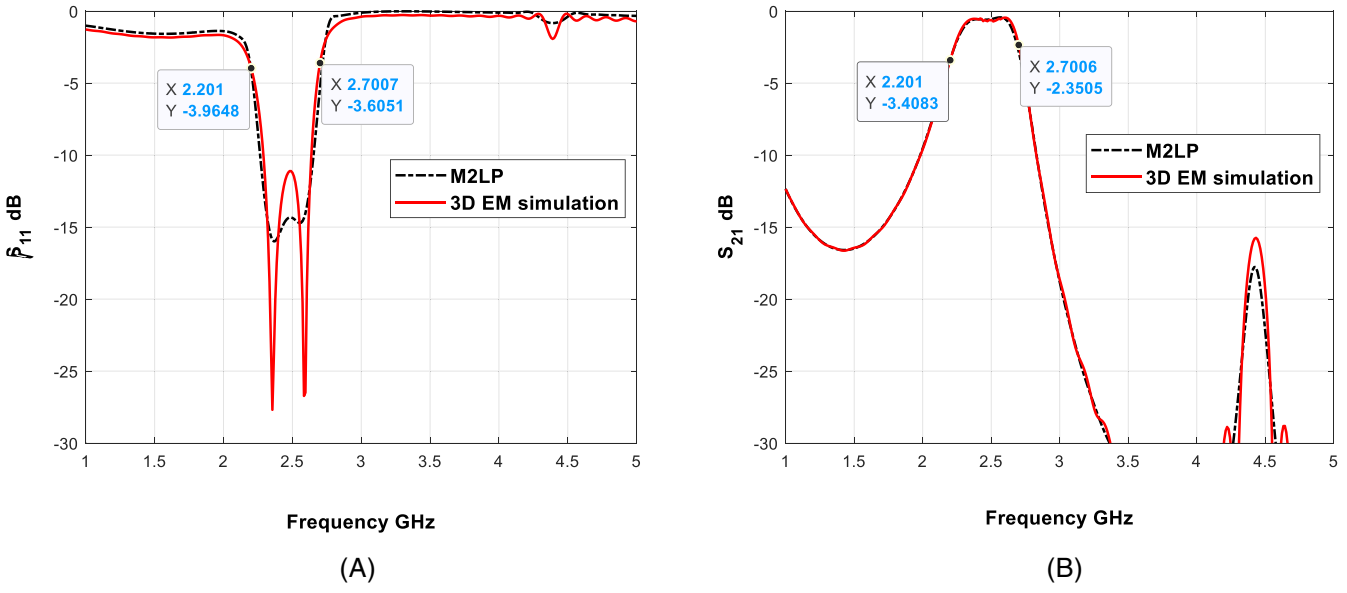

FIGURE 9 Simulated (A) S_{11}, (B) S_{21}, results of CST and M2LP-based 7 element NTL filter

For the last decades, meta-heuristic algorithms (MHA) have been extensively used as an effective direct search tool in design optimization process of many linear and nonlinear microwave stages.[33,63-73] Thanks to their unique heuristic-based search algorithms that do not require a differential operator, these algorithms can be efficiently used for solving nondifferentiable or discontinuous, nonconvex, and highly nonlinear problems that might not be solved with gradient-based algorithms.

Differential evolutionary algorithm (DEA) is a multidimensional optimization algorithm from the evolutionary algorithm class. DEA is originated by Kenneth Price and Rainer M. Storn, and first publication of idea of this method was published as a technical report in References 77 and 78. DEA is a population-based MHA in which members of population (candidate solutions) are improved iteratively via the use of recombination, evaluation, and selection. In recombination, new individuals (offspring) are introduced to the system, by using the weighted difference of two members (parents); usually this selection is randomized. In conjunction with selection, the perturbation effect self-organizes

the sampling of the problem space, bounding it to known areas of interest.[74-79] Recently, DEA has shown great potential in solving of complex microwave circuit design optimizations.[2,68,69,80-83]

At this point, an efficient optimization tool, DEA, has been used for solving the M2LP-based NTL filter design optimization problem. The limitation of optimization variables is taken equal to the limitation in Table 1. Following user defined parameters have been used for DEA search: Maximum iteration = 30, population = 50, scale factor = 0.25, cross-over = 0.5, and $cost_{Req} = 0$. In Table 5, the optimal design values of the 7 element NTL filter have been presented; here, the values obtained from DEA are rounded with respect to prototyping error tolerance of "50 μm" with PCB milling technology.

For justification of the obtained M2LP results, the obtained optimal parameters are used to model a 3D model of the proposed NTL filter in CST environment. The CST-based model has been presented in Figure 8 alongside of its simulated results in Figure 9. As can be seen, the proposed design optimization process had achieved hand-to-hand results with 3D EM simulation tool.

4 | CONCLUSIONS

Herein, by using M2LP model a fast, accurate surrogate modeling of a nonuniform microstrip transmission line (NTL) had been achieved. Different sampling methods are used for generating the training and test data sets. Then, the proposed M2LP NTL model has been used as a unit element for design optimization of a band-pass filter for ISM band applications. In this study, M2LP model has been compared with counterpart regression model in terms of performance. As a consequence, the proposed method is more accurated in terms of cross-validation and hold out performances. The optimal determination of geometrical design parameters, which are also the input variables of M2LP model, of cascaded NTL's is taken as a multi-objective multidimension optimization problem to be solved via the use of meta-heuristic optimization algorithm DEA. The obtained results are justified with a 3D EM simulated model of the proposed NTL filter in CST environment. As it can be seen from the results, the proposed M2LP NTL model can be used not only for design of nonuniform microwave filters but also for design of other microwave circuit stages by simply changing the design optimization objective.

ACKNOWLEDGEMENT

We would like to express our special thanks of gratitude to the Aktif Neser Elektronik, for providing researcher license of CST.

DATA AVAILABILITY STATEMENT

Data available on request from the authors.

ORCID

Tarlan Mahouti https://orcid.org/0000-0001-5178-4878

REFERENCES

1. Mahouti P. Application of artificial intelligence algorithms on modeling of reflection phase characteristics of a nonuniform reflectarray element. *Int J Numer Model*. 2020;33(2):e2689.
2. Koziel S, Pietrenko Dabrowska A. Design-oriented computationally-efficient feature-based surrogate modelling of multi-band antennas with nested kriging. *AEU Int J Electron Commun*. 2020;120:153202.
3. Koziel S, Ogurtsov S. *Simulation-Based Optimization of Antenna Arrays*. Singapore: World Scientific; 2019.
4. Sóbester A, Forrester AIJ, Toal DJJ, Tresidder E, Tucker S. Engineering design applications of surrogate-assisted optimization techniques. *Optim Eng*. 2014;15:243-265. https://doi.org/10.1007/s11081-012-9199-x.
5. Zhang W, Yan S, Feng F, Zhang Q. Fast and simple technique for computing circuit noise figure from component noise model using artificial neural network. Paper presented at: 2015 IEEE MTT-S NEMO (pp. 1-3).
6. Chávez-Hurtado JL, Rayas-Sánchez JE. Polynomial-based surrogate modeling of RF and microwave circuits in frequency domain exploiting the multinomial theorem. *IEEE Trans Microw Theory Tech*. 2016;64(12):4371-4381. https://doi.org/10.1109/TMTT.2016.2623902.
7. Jin J, Zhang C, Feng F, Na W, Ma J, Zhang QJ. Deep neural network technique for high-dimensional microwave modeling and applications to parameter extraction of microwave filters. *IEEE Trans Microw Theory Tech*. 2019;67(10):4140-4155. https://doi.org/10.1109/TMTT.2019.2932738.
8. Lophaven SN, Nielsen HB, Søndergaard J, Dace A. A Matlab kriging toolbox. Tech: University of Denmark. 2002.
9. Gorissen D, Crombecq K, Couckuyt I, Dhaene T, Demeester P. A surrogate modeling and adaptive sampling toolbox for computer based design. *J Mach Learn Res*. 2010;11:2051-2055.
10. Marelli S, Sudret B. UQLab: A framework for uncertainty quantification in Matlab. Paper presented at: Int. Conf. Vulner. Risk Analysis Manag. (ICVRAM), Liverpool, United Kingdom, July 2014, p. 2554–63.

11. Hassan AKS, Etman AS, Soliman EA. Optimization of a novel nano antenna with two radiation modes using kriging surrogate models. *IEEE Photon J*. 2018;10(4):1-17. https://doi.org/10.1109/JPHOT.2018.2848593.
12. Dong J, Li Q, Deng L. Fast multi-objective optimization of multi-parameter antenna structures based on improved MOEA/D with surrogate-assisted model. *AEU Int J Electron Commun*. 2017;72:192-199.
13. Mishra S, Yadav RN, Singh RP. Directivity estimations for short dipole anten-na arrays using radial basis function neural networks. *IEEE Antent Wireless Propag Lett*. 2015;14:1219-1222. https://doi.org/10.1109/LAWP.2015.2399453.
14. Jacobs JP. Efficient resonant frequency modeling for dual-band microstrip antennas by gaussian process regression. *IEEE Anten Wireless Propag Lett*. 2015;14:337-341. https://doi.org/10.1109/LAWP.2014.2362937.
15. Rayas-Sánchez JE. EM-based optimization of microwave circuits using artificial neural networks: the state-of-the-art. *IEEE Trans Microw Theory Tech*. 2004;52(1):420-435. https://doi.org/10.1109/TMTT.2003.820897.
16. Feng F, Zhang C, Ma J, Zhang QJ. Parametric modeling of EM behavior of microwave components using combined neural networks and pole-residue-based transfer functions. *IEEE Trans Microw Theory Tech*. 2016;64(1):60-77. https://doi.org/10.1109/TMTT.2015.2504099.
17. Kabir H, Wang Y, Yu M, Zhang Q-J. Neural network inverse modeling and applications to microwave filter design. *IEEE Trans Microw Theory Tech*. 2008;56(4):867-879. https://doi.org/10.1109/TMTT.2008.919078.
18. Prado DR, López-Fernández JA, Arrebola M, Goussetis G. Support vector regression to accelerate design and crosspolar optimization of shaped-beam reflectarray antennas for space applications. *IEEE Trans Anten Propag*. 2019;67(3):1659-1668. https://doi.org/10.1109/TAP.2018.2889029.
19. Jacobs JP. Bayesian support vector regression with automatic relevance determination kernel for modeling of antenna input characteristics. *IEEE Trans Anten Propag*. 2012;60(4):2114-2118. https://doi.org/10.1109/TAP.2012.2186252.
20. Easum JA, Nagar J, Werner DH. Multi-objective surrogate-assisted optimization applied to patch antenna design. Paper presented at: IEEE Int. Symp. Ant. Prop. (APS/URSI), San Diego, CA, July 2017. pp. 339–340.
21. Gehani A, Agnihotri P, Pujara DA. Analysis and synthesis of multiband Sierpinski carpet fractal antenna using hybrid neuro-fuzzy model. *Prog Electromag Res Lett*. 2017;68:59-65. https://doi.org/10.2528/PIERL16100701.
22. Wu X, Peng X, Chen W, Zhang W. A developed surrogate-based optimization framework combining HDMR-based modeling technique and TLBO algorithm for high dimensional engineering problems. *Struct Multidiscip Optim*. 2019;60(2):663-680. https://doi.org/10.1007/s00158-019-02228-4.
23. Mahouti P. Design optimization of a pattern reconfigurable microstrip antenna using differential evolution and 3D EM simulation-based neural network model. *Int J RF Microw Comp Aided Eng*. 2019;29(8):e21796.
24. Giannini F, Leuzzi G, Orengo G, Albertini M. Small-signal and large-signal modeling of active devices using CAD-optimized neural networks. *Int J RF Microw Comp Aided Eng*. 2002;12(1):71-78. https://doi.org/10.1002/mmce.10007.
25. Marinković ZD, Marković VV. Temperature-dependent models of low-noise microwave transistors based on neural networks. *Int J RF Microw Comp Aided Eng*. 2005;15(6):567-577. https://doi.org/10.1002/mmce.20102.
26. Gunes F, Mahouti P, Demirel S, Belen MA, Uluslu A. Cost-effective GRNN-based modeling of microwave transistors with a reduced number of measurements. *Int J Numer Model*. 2017;30(3-4):e2089. https://doi.org/10.1002/jnm.2089.
27. Gunes F, Belen MA, Mahouti P, Demirel S. Signal and Noise Modeling of Microwave Transistors Using Characteristic Support Vector-based Sparse Regression. *Radioengineering*. 2016;25(3):490-499. https://doi.org/10.13164/re.2016.0490.
28. Marinković Z, Crupi G, Caddemi A, Marković V, Schreurs DMMP. A review on the artificial neural network applications for small-signal modeling of microwave FETs. *Int J Numer Model*. 2020;33:e2668. https://doi.org/10.1002/jnm.2668.
29. Mahouti M, Kuskonmaz N, Mahouti P, Belen MA, Palandoken M. Artificial neural network application for novel 3D printed non-uniform ceramic reflectarray antenna. *Int J Numer Model*. 2020;33:e2746. https://doi.org/10.1002/jnm.2746.
30. Güneş F, Demirel S, Nesil S. A novel design approach to X-band Minkowski reflectarray antennas using the full-wave EM simulation-based complete neural model with a hybrid GA-NM algorithm. *Radioengineering*. 2014;23(1):144-153.
31. Mahouti P, Gunes F, Caliskan A, Belen MA. A novel design of non-uniform reflectarrays with symbolic regression and its realization using 3-D printer. *ACES*. 2019;34(2):280-285.
32. Krishna D, Narayana J, Reddy D. ANN models for microstrip line synthesis and analysis. *Int J Elect Syst Sci Eng*. 2008;1(3):196-200.
33. Günes F, Demirel S, Mahouti P. Design of a front–end amplifier for the maximum power delivery and required noise by HBMO with support vector microstrip model. *Radioengineering*. 2014;23(1):134-143.
34. Mahouti P, Güneş F, Belen MA, Demirel S. Symbolic regression for derivation of an accurate analytical formulation using "big data": an application example. *ACES*. 2017;32(5):372-380.
35. Karaboga D, Guney K, Sagirogl S, Erler M. Neural computation of resonant frequency of electrically thin and thick rectangular microstrip antennas. *IEE Proc Microw Anten Propag*. 1999;146:155-159. https://doi.org/10.1049/ip-map:19990136.
36. Mishra RK, Patnaik A. Neural network-based CAD model for the design of square patch antennas. *IEEE Trans Anten Propag*. 1998;46:1890-1891. https://doi.org/10.1109/8.743842.
37. Ambasana N, Anand G, Gope D, Mutnury B. S-parameter and frequency identification method for ANN-based eye-height/width prediction. *IEEE Trans Compon, Packag Manufact Technol*. 2017;7(5):698-709. https://doi.org/10.1109/TCPMT.2017.2661065.
38. Koziel S, Bekasiewicz A. Computationally feasible narrow-band antenna modeling using response features. *Int J RF Microw Comput Aided Eng*. 2017;27(4):e21077. https://doi.org/10.1002/mmce.21077.
39. Koziel S, Bekasiewicz A. Expedited simulation-driven design optimization of UWB antennas by means of response features. *Int J RF Microw Comput Aided Eng*. 2017;27(6):1-8.
40. Tu S, Cheng QS, Zhang Y, Bandler JW, Nikolova NK. Space mapping optimization of handset antennas exploiting thin-wire models. *IEEE Trans Anten Propag*. 2013;61(7):3797-3807. https://doi.org/10.1109/TAP.2013.2254695.

41. Koziel S, Bekasiewicz A, Couckuyt I, Dhaene T. Efficient multi-objective simulation-driven antenna design using co-kriging. *IEEE Trans Anten Propag*. 2014;62(11):5900-5905. https://doi.org/10.1109/TAP.2014.2354673.
42. Koziel S. Low-cost data-driven surrogate modeling of antenna structures by constrained sampling. *IEEE Ant Wireless Propag Lett*. 2017; 16:461-464. https://doi.org/10.1109/LAWP.2016.2583474.
43. Koziel S, Pietrenko Dabrowska A. Performance-based nested surrogate modeling of antenna input characteristics. *IEEE Trans Anten Propag*. 2019;67(5):2904-2912. https://doi.org/10.1109/TAP.2019.2896761.
44. Calik N, Belen MA, Mahouti P. Deep learning base modified MLP model for precise scattering parameter prediction of capacitive feed antenna. *Int J Numer Model*. 2020;33:e2682.
45. Zhu W, Huang Y, Zeng L, et al. AnatomyNet: deep learning for fast and fully automated whole-volume segmentation of head and neck anatomy. *Med Phys*. 2019;46(2):576-589. https://doi.org/10.1002/mp.13300.
46. Liu F, Zhou Z, Jang H, Samsonov A, Zhao G, Kijowski R. Deep convolutional neural network and 3D deformable approach for tissue segmentation in musculoskeletal magnetic resonance imaging. *Magn Reson Med*. 2018;79(4):2379-2391.
47. Zhang B, Li S, Huang Z, Rahi BH, Wang Q, Li M. Transfer learning-based online multiperson tracking with Gaussian process regression. *Concurr Comput*. 2018;30(23):e4917. https://doi.org/10.1002/cpe.4917.
48. Son J, Baek M, Cho M, Han B, Multi-object tracking with quadruplet convolutional neural networks. Paper presented at: Proceedings of the IEEE conference on Comp. vis. and Patt. Rec. (pp. 5620-5629).
49. Moazzen Y, Çapar A, Albayrak A, Çalık N, Töreyin BU. Metaphase finding with deep convolutional neural networks. *Biomed Signal Process Control*. 2019;52:353-361. https://doi.org/10.1016/j.bspc.2019.04.017.
50. Albayrak A, Unlu A, Calik N, et al. A Whole Slide Image Grading Benchmark and Tissue Classification for Cervical Cancer Precursor Lesions with Inter-Observer Variability. arXiv preprint arXiv:1812.10256 2018.
51. Chung JS, Zisserman A. Lip reading in the wild. *Asian Conference on Computer Vision*. Cham: Springer; 2016.
52. Zeng M, Nguyen LT, Yu B, et al.. Convolutional neural networks for human activity recognition using mobile sensors. Paper presented at: 6th Int. Conf. on Mobile Comp., App. and Services (pp. 197-205). IEEE.
53. Babu GS, Zhao P, Li XL. Deep convolutional neural network based regression approach for estimation of remaining useful life. Paper presented at: Int. conf. on database systems for adv. App (pp. 214-228). Springer, Cham.
54. Bao W, Yue J, Rao Y. A deep learning framework for financial time series using stacked autoencoders and long-short term memory. *PLoS One*. 2017;12(7):e0180944.
55. Qureshi AS, Khan A, Zameer A, Usman A. Wind power prediction using deep neural network based meta regression and transfer learning. *Appl Soft Comput*. 2017;58:742-755.
56. Li Y, Shi H, Han F, Duan Z, Liu H. Smart wind speed forecasting approach using various boosting algorithms, big multi-step forecasting strategy. *Renew Energy*. 2019;135:540-553.
57. Wei Z, Liu D, Chen X. Dominant-current deep learning scheme for electrical impedance tomography. *IEEE Trans Biomed Eng*. 2019;66 (9):2546-2555.
58. Wei Z, Chen X. Deep-learning schemes for full-wave nonlinear inverse scattering problems. *IEEE Trans Geosci Remote Sens*. 2019;57(4): 1849-1860. https://doi.org/10.1109/TGRS.2018.2869221.
59. Calik N, Kurban OC, Yilmaz AR, Yildirim T, Ata LD. Large-scale offline signature recognition via deep neural networks and feature embedding. *Neurocomputing*. 2019;359:1-14. https://doi.org/10.1016/j.neucom.2019.03.027.
60. Li B, Jiao B, Chou CH, Mayder R, Franzon P. Self-evolution cascade deep learning model for high-speed receiver adaptation. *IEEE Trans Compon Packaging Manuf Technol*. 2020;10:1043-1053.
61. Jing J, Feng F, Zhang J, Yan S, Na W, Zhang QJ. A novel deep neural network topology for parametric modeling of passive microwave components. *IEEE Access*. 2020;8:82273-82285.
62. Pozar DM. *Microwave Engineering*. 3rd ed. Hoboken, NJ: J. Wiley; 2005.
63. Güneş F, Demirel S, Mahouti P. A simple and efficient honey bee mating optimization approach to performance characterization of a microwave transistor for the maximum power delivery and required noise. *Int J Numer Model*. 2016;29(1):4-20.
64. Zheng SY. The applications of jumping genes inspired evolutionary algorithms in microwave circuit designs. Paper presented at: 2017, Int. Symp. ACES, Suzhou. 2017, pp. 1-2.
65. Güney K, Onay M. Bees algorithm for design of dual- beam linear antenna arrays with digital attenuators and digital phase shifters. *Int J RF Microw CAE*. 2008;18:337-347. https://doi.org/10.1002/mmce.20292.
66. Galehdar A, Thiel DV, Lewis A, Randall M. Multi objective optimization for small meander wire dipole antennas in a fixed area using ant colony system. *Int J RF Microw Comput Aided Eng*. 2009;19:592-597. https://doi.org/10.1002/mmce.20382.
67. Zheng SY, Yeung SH, Chan WS, Man KF, Tang KS. Design of broadband hybrid coupler with tight coupling using jumping gene evolutionary algorithm. *IEEE Trans Ind Electron*. 2009;56(8):2987-2991. https://doi.org/10.1109/TIE.2009.2020080.
68. Güneş F, Belen MA, Mahouti P. Competitive evolutionary algorithms for building performance database of a microwave transistor. *Int J Circ Theor Appl*. 2018;46(2):244-258. https://doi.org/10.1002/cta.2386.
69. Yıldırım A, Güneş F, Belen MA. Differential evolution optimization applied to the performance analysis of a microwave transistor. *Sigma J Eng Nat Sci*. 2017;8(2):135-144.
70. Clark H, Jeong NS, Jeong S. Concurrent Gain and Bandwidth Improvement of a Patch Antenna with a Hybrid Particle Swarm Optimization Algorithm. Paper presented at: 2019 IEEE 20th WAMICON, Cocoa Beach, FL, USA, 2019. pp. 1-3.
71. Rahmat-Samii Y. Modern Antenna Designs using Nature Inspired Optimization Techniques: Let Darwin and the bees help designing your Multi band MIMO antennas. Paper presented at: 2007 IEEE Radio and Wireless Symposium, pp. 463-466, 2007.

72. Patel P, Kumari G, Saxena P. Array Pattern Correction in Presence of Antenna Failures using Metaheuristic Optimization Algorithms. Paper presented at: 2019 Int. Conf. on Comm. and Signal Process. (ICCSP), Chennai, India, 2019, pp. 0695-0700.
73. Grewal NS, Rattan M, Patterh MS. A linear antenna array failure detection using Bat algorithm. Paper presented at: IEEE Inter Conf on Contemp Comput pp. 202-207, 2015.
74. Storn R, Price K. Differential Evolution: A Simple and Efficient Adaptive Scheme for Global Optimization over Continuous Spaces. Technical Report TR-95-012, Int. Computer Science Institute, Berkeley, CA, 1995.
75. Storn R. On the Usage of Differential Evolution for Function Optimization. Paper presented at: Proceedings Fuzzy Information Processing Society, 1996 Biennial Conference of the North American, 1996.
76. Storn R. Differential evolution design of an IIR-filter. IEEE Conf. Evo. Comput. 1996.
77. Storn R, Price K. Minimizing the real functions of the ICEC'96 contest by differential evolution. IEEE Conf. Evo. Comput. 1996.
78. Storn R, Price K. Differential evolution: a simple and efficient heuristic for global optimization over continuous spaces. *J Glob Optim*. 1997;11:341-359.
79. Lampinen J, Storn R. Differential Evolution. *New Optimization Techniques in Engineering*. Studies in Fuzziness and Soft Computing 141. Berlin, Heidelberg: Springer. 2004. https://doi.org/10.1007/978-3-540-39930-8_6.
80. Li X, Yin M. Design of a reconfigurable antenna array with discrete phase shifters using differential evolution algorithm. *Prog Electromagn Res B*. 2011;31:29-43. https://doi.org/10.2528/PIERB11032902.
81. Li X, Yin M. Hybrid differential evolution with biogeography-based optimization for design of a reconfigurable antenna array with Discrete phase shifters. *Int J Anten Propag*. 2011;2011:685629. https://doi.org/10.1155/2011/685629.
82. Li X, Yin M. Design of multi objective reconfigurable antenna array with discrete phase shifters using multiobjective differential evolution based on decomposition. *Int J RF Microw Comp Aid Eng*. 2012;22:675-681. https://doi.org/10.1002/mmce.20626.
83. Rao AP, Sarma NVSN. Synthesis of reconfigurable antenna array using differential evolution algorithm. *IETE J Res*. 2017;63(3):428-434. https://doi.org/10.1080/03772063.2017.1284614.

AUTHOR BIOGRAPHIES

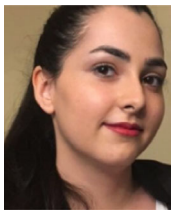

Tarlan Mahouti received her BSc degree in Metallurgy and Material Science Engineering from the Yıldız Technical University in 2018. Currently, she is an MSc student in Yıldız Technical University. Her current activities include material and system modeling simulation and validation along with Development of Artificial Intelligence Algorithms for design optimization process. Her current research interests are in the areas of computer science and information technology.



Tülay Yildirim (Member, IEEE) received the BSc and MSc degrees in electronics and communication engineering from Yildiz Technical University, Istanbul, Turkey, in 1990 and 1992, respectively, and the PhD degree in electrical and electronics engineering from the University of Liverpool, UK, in 1997. She is currently a Full Professor with the Department of Electronics and Communications Engineering, Yildiz Technical University. She has authored over 200 publications in journals, conferences, and books. Her research interests include artificial intelligence, intelligent systems, cyber-physical systems, biomedical instrumentation, biometric person identification, and verification systems.



Nilgün Kuşkonmaz received her MSc and the PhD degrees in Metallurgy and Material Science Engineering from the Istanbul Technical University in 1983 and 1992. Currently, she is a Full Professor in Yildiz Technical University. Her current activities include material science research and advanced ceramics. Her current research interests are in the areas of nanotechnology, tape casting with Dr. Blade, and advanced ceramic modeling.

How to cite this article: Mahouti T, Yıldırım T, Kuşkonmaz N. Artificial intelligence–based design optimization of nonuniform microstrip line band pass filter. *Int J Numer Model*. 2021;e2888. https://doi.org/10.1002/jnm.2888